Cellulose (2023) 30:4041–4055
https://doi.org/10.1007/s10570-023-05125-8

ORIGINAL RESEARCH

# Imparting cotton textiles glow-in-the-dark property along with other functional properties: photochromism, flame-retardant, water-repellency, and antimicrobial activity

**Esraa Ahmed · Dalia Maamoun · Meram S. Abdelrahman · Talaat M. Hassan · Tawfik A. Khattab**

Received: 30 December 2022 / Accepted: 28 February 2023 / Published online: 14 March 2023


**Abstract** Screen-printing and spray-coating methods were used to produce photoluminescent, water-repellent, and antimicrobial films on textile fibers. The cotton fabrics were firstly finished with a flame-resistant agent. There are a number of functional agents that have been applied during the textile finishing process, including strontium aluminate pigment as antibacterial and photoluminescent agent, flame-retardant organophosphate, and water-repellent silicone rubber. The current research investigated the surface morphologies and chemical compositions of the screen-printed and spray-coated fabric cottons using scanning electron microscopy (SEM), transmission electron microscopy (TEM), energy-dispersive X-ray (EDX), wavelength dispersive X-ray fluorescence (WDXRF), and Fourier-transform infrared spectroscopy (FT-IR). According to morphological analysis, the phosphor nanoparticles had sizes ranging from 2 to 12 nm. After excitation at 399 nm, the generated colorless photoluminescent layer deposited onto cotton surface showed an emission profile at 516 nm. The luminescence spectra and CIE Lab characteristics confirmed that the phosphor-coated textiles displayed a white color in visible spectrum and green emission in the presence of UV light. It has been shown by analysis that the tested colors are very stable over time. The measurements of static water contact and sliding angles were also explored. The self-extinguishing activity of the coated fabrics retained their flame-retardant properties over 24 laundry cycles. Antimicrobial activity, hydrophobicity, and luminous properties were improved without affecting the intrinsic physical and mechanical features of the treated textiles. Details on the CIE Lab colorimetric measurements were discussed. The stiffness and air permeability were examined to explore the flexibility and breathability of the treated textile fibers. Excellent reversibility and photostability were seen in the phosphor-coated materials.

**Keywords** Cotton fabric · $SrAl_2O_4:Eu^{2+}, Dy^{3+}$ · Flame-retardant · Phosphorescence · Water-repellency · Antibacterial

E. Ahmed · T. M. Hassan
Department of Technical and Industrial Education, Faculty of Education, Helwan University, Cairo, Egypt

D. Maamoun
Printing, Dyeing and Finishing Department, Faculty of Applied Arts, Helwan University, Cairo 11795, Egypt

M. S. Abdelrahman · T. A. Khattab (✉)
Dyeing, Printing and Auxiliaries Department, Textile Research and Technology Institute, National Research Centre, Cairo 12622, Egypt
e-mail: ta.khattab@nrc.sci.eg

## Introduction

As the need for textiles in technological applications grows, products with a single purpose are no longer adequate. The use of a variety of functional fabrics

has been crucial in delivering the required qualities. This is why researchers have been focusing on creating textiles with multifunctional uses (Meena et al. 2022; Roach et al. 2019; Tat et al. 2022). The key functions of smart textiles include photochromism, self-cleaning, antimicrobial and superhydrophobic properties. Manufacturers of multifunctional textiles have focused on the development of innovative strategies to expand the applications of the renewable and ecologically benign fibrous materials (Chen et al. 2020; De Falco et al. 2019). Textile materials have been known to promote microbial growth owing to their high capacity to absorb moisture (Wang et al. 2022). In order to make textiles more versatile, several different organic compounds have been utilized. Environmental toxicity and high production costs are only two of the many problems that have been discovered with textiles treated using traditional organic substances like fluorocarbons and triclosan (Zhang et al. 2019). A single processing step has been used to provide textiles with a singular practical quality. Thus, a fabric undergoes numerous finishes to be imparted multiple functions, which require more time and resources (Faruk et al. 2021). Metal-based nanoparticles can be achieved quickly in textile finishing by employing several smart materials to finish the textiles. In recent investigations, it was shown that metal-based nanoparticles have considerable potential for producing high-value textile products without degrading textile look or mechanical qualities. Functional technological textiles fall into a variety of categories, such as sportswear, construction, medical, hygiene, transportation, and agriculture (Fang et al. 2021; Shi et al. 2019; Tadesse et al. 2019).

Smart clothing can help with muscle vibration management, topical drug delivery, and temperature control agents. Smart textiles can change color, and even display images, videos, and light patterns. Smart clothing relies on three main elements, including sensors, actuators, and controls (Fan et al. 2020; He et al. 2020; Khattab et al. 2018). The production processes of traditional textiles include laminating, weaving, and knitting. Those processes have been also applied to produce smart multifunctional textiles. The integration of electronic parts into clothing is possible via the use of portable electronic devices that can be sewn into, sewed onto, or otherwise attached to the fabric. Electric fields, light and heat are some examples of the external stimuli that smart fibers can respond to to demonstrate a greater chance of enhancing their protective capabilities (Fan et al. 2022; Sun et al. 2020). Photochromic textile can change color upon exposure to light (Yang et al. 2021). Sunglasses, memory, ophthalmic lenses, packaging, sensors and displays are among the many documented applications of photochromic materials. Producing photochromic materials must not sacrifice their design, care, low cost, sensing activity, wearability, flexibility, and tensile strength (Ahmed et al. 2022; Bao et al. 2020; Gao et al. 2022a, b). The color of fabrics made from photochromic fibers changes in response to exposure to either visible light or ultraviolet radiation. Different dyes have been used to make chromic textiles that change color in the presence of light (Alsharief et al. 2022). Spirooxazines and other organic light-induced chromic dyestuffs have been used to develop photochromic textiles. In many cases, the quantity of organic dyestuffs that can be absorbed by textile fibers decreases as a consequence of degradation during the color finishing process (Gao et al. 2022a, b). There is also a possibility that the material fibrous mass might reduce the photochromic performance of the organic dyestuffs due to the fibrous bulk rigidity. Thus, photochromic organic dyes usually exhibit poor colorfastness properties to light and washing. Moreover, the fabrics treated with organic dyes tend to become stiffer and rougher. Because of their low thermal and photostabilty and higher cost relative to inorganic pigments, organic colorants usually have limited applications (Yuan et al. 2019; Zampini et al. 2022). Cotton fabrics have found many uses in diverse fields, including medical, furniture, automotive, and foodstuff packaging industries (Gao et al. 2021; Kibria et al. 2022; Wei et al. 2020). Cotton fabrics are inexpensive with good flexural and impact strengths. They are characterized with softness, durability, absorbency, holds dye well, and breathability. Cotton is mainly composed of cellulose, which is renewable, biodegradable, and naturally abundant (Subaihi et al. 2022).

Both screen-printing and spray-coating have been reported as excellent textile coating technologies because they are appropriate methods for incorporating low ratios of pigment particles into the surface of textile materials (Gong et al. 2018; Lamas-Ardisana et al. 2018). Herein, we apply the screen-printing and spray-coating to immobilize lanthanide-doped strontium aluminate particles (photoluminescent

agent), flame-retardant organophosphate and water-repellent silicone rubber onto cotton fibers to create smart textiles with enhanced properties such as color-changing ability, durability, photostability, superhydrophobicity, UV protection, flame-retardant activity, good colorfastness, antimicrobial activity, and comfortability.

## Experimental

### Materials

El-Mahalla textiles Company (El-Mahalla, Egypt) generously provided cotton (100%) textile substrates. Dystar (Egypt) provided the thickener (Alcoprint PTP) and Binder additive. Sigma-Aldrich was the source for the $Al_2O_3$, $Eu_2O_3$, $H_3BO_3$, $Dy_2O_3$, and $SrCO_3$ (Egypt). Decoseal-2540 (silicone rubber) was purchased from ADMICO (Egypt). Exolit-AP422 (ammonium polyphosphate) was purchased from Shandong Shi'an (China).

### Synthesis of pigment microparticles

The high temperature solid state approach (El-Newehy et al. 2022) was applied to synthesize the inorganic pigment ($SrAl_2O_4$:$Eu^{2+}$, $Dy^{3+}$). A dispersion of Dy(III) oxide, Sr(II) carbonate, Eu(III) oxide, aluminum oxide, and boric acid in ethanol was ultrasonicated for 30 min, heated at 90 °C for 20 h, then grinded for 2 h. The resulting particles was sintered at 1300 °C for about 2.5 h, milled, and sieved to produce the inorganic pigment microparticles (12–28 µm).

### Synthesis of pigment nanoparticles

The top-down method (Camargos and Rezende 2021) was used to create the pigment nanoparticles, in which 10 g of the pigment phosphor microparticles were loaded into a ball mill tube (20 cm in diameter) connected to a vibrate plate. In order to create the pigment phosphor nanoparticles, a SiC ball mill (0.1 cm) was allowed to repetitively strike with the vibrating plate and the tube containing the pigment powder for 23 h.

### Fabrication of luminescent fabrics by screen-printing (SP)

Diammonium phosphate (0.1%), ammonium hydroxide (0.1%), ammonium polyphosphate (10%), and binding agent (15%) were combined with water to produce the printing stock paste. It was then mixed for 10 min to enable complete viscosity to form with the addition of the synthetic thickening alcoprint PTP (2%). When the mixture had been stirred for 15 min, phosphor pigment (1% ($SP_1$), 5% ($SP_2$), 10% ($SP_3$), and 15% ($SP_4$) w/w) was added. When the viscosity of the printing paste decreased below 21,000 cps at a shearing rate of 2.20, the printing paste was allowed to thicken by adding a little quantity of thickener. The screen-printing technology was utilized to deposit the printing paste on cotton fibers. Thermal fixing was performed at 160 °C for four minutes on the final printed materials after they had been dried at room temperature (Werner Mathis; Switzerland). It was rinsed with hot water at 50 °C, washed with tap water, and lastly air-dried.

### Preparation of photoluminescent fabrics by spray-coating (SC)

RTV (15% w/v) and ammonium polyphosphate (100 g/L) were dispersed in petroleum ether by stirring for an hour. The phosphor nanopowder was then added at different concentrations; including 1% ($SC_1$), 5% ($SC_2$), 10% ($SC_3$), and 15% ($SC_4$) w/w. Every admixture was stirred for 2 h, and homogenization (25 kHz) for 20 min. The spray-coating process was performed at a flowing rate of 10 mL/minute utilizing automatic Lumina spraying gun (STA6R; Fuso Seiki, Japan). The spray nozzle (orifice size of 1 mm)) was wagged back and forth (rate of 3 cm $s^{-1}$) at a distance of 20 cm from the cotton fabric. The spray-coating process was performed till reaching a complete coating of sample. The fabric was air-dried for 30 min. Figure 1 displays a schematic diagram demonstrating the finishing procedures of multifunctional textiles via screen-printing and spray-coating technologies.

### Characterization methods

#### *Photoluminescence screening*

All measurements were performed in a laboratory using a standard set of environmental parameters. For


**Fig. 1** Diagram demonstrates the preparation of multifunctional textiles via screen-printing and spray-coating technologies

the phosphorescence measurements, the coated cotton textiles were analyzed using a JASCO FP-6500 (Japan), which was fitted with phosphorescence accessories for measuring the lifetime spectra. Both phosphorescence measurements were conducted under the identical geometrical circumstances. The monochromators use Xenon Arc Lamp (150 W) with slit bandwidths of 5 nm. Excitation and emission spectra were modified to take into account the features of the emission monochromator and photomultiplier response of the instrument. Phosphorescence emission and excitation spectra were measured by stimulation at the maximum wavelength of phosphorescence absorption. The irradiation was carried out using UV supply (365 nm, 6 W).

*Reversibility of coated cotton*

The coated samples luminescent properties and technical behavior were investigated using previous procedures (Abou-Melha 2022). The fabrics were subjected to UV illumination for 5 min followed by 60 min of darkness to allow the stored light to dissipate and return to its original condition. Over the course of 15 cycles, the irradiation-fading performance was replicated. After each cycle, the phosphorescence emission was obtained.

*Colorimetric measurements*

The colorimetric measurements were collected before and after UV illumination employing the CIE Lab coordinate according to previous procedures (Khattab et al. 2021). The fabrics were subjected to UV illumination for 5 min at a distance of 4 cm from the UV lamp (365 nm and 6 Watt). The ultraviolet lamp was switched off and the colorimetric parameters were immediately reported.

*Morphological properties*

The phosphor particle shape and size was reported by JEOL 1230 TEM (Japan). The phosphor particles were suspended in acetone and ultrasonicated (25 kHz) for 30 min for TEM analysis. Nexus 670 FTIR (Nicolet, USA) was utilized to investigate the functional substituents on fabric surface. Quanta FEG 250 SEM (Republic of Czech) was utilized to examine the morphological features paired with an EDX spectroscope. The EDX diagrams were recorded at an accelerating voltage of 20 kV.

*Comfort screening*

Shirley stiffness apparatus was employed to determine the bend length of the untreated (pristine) and treated cotton samples according to British standard procedure 3356:1961 (Thite et al. 2018). A pressure gradient of 100 Pa was used to evaluate the permeability of fabric to air using an FX-3300 Textest under the ASTM D737 standardized protocol (Adamu 2022). There were five measurements taken for each sample to get an average of bend length and air permeability results.

*Hydrophobicity study*

Dataphysics OCA15EC (Germany) was employed to determine the static contact angles (Wongphan and Harnkarnsujarit 2020).

*UV-protection evaluation*

Previous procedures (Hu et al. 2022) were used to determine the UPF (UV Protection Factor) using the standard 4399 (1996) AS/NZS protocol under the standard AATCC(183:2010) protocol to report

the effectiveness of the coated textiles to block UV light.

*Flammability tests*

Under the standard vertical flammability test method of BS 5438:1989; Test 2B was utilized to evaluate the flame-retardant activity of samples (10×40 cm). After measuring the char length (mm), the fabrics were washed over several laundry cycles up to 24 in accordance with AATCC 61:1989. The multifunctional fabric was inserted into a launder-o-meter accelerated machine. A detergent solution (200 mL) was charged into the laundry machine at 40±3 °C for 45 min. The flame-retardant durability was evaluated by measuring the char length after every laundry cycle (El-Naggar et al. 2022). Additionally, the limited oxygen index (LOI) chamber was applied to evaluate the flame-retardant performance of the treated cotton fabrics according to ISO:4589-1 (2017) and ASTM D2863 standard tests (Abd El-Wahab et al. 2020).

*Biological activity*

The AATCC (1999) 100 protocol and the plate agar counting method were utilized to report the antimicrobial activity of the coated cottons against *S. typhimurium* (ATCC: 14,028) and *S. aureus* (ATCC: 25,923) (Shen et al. 2022). Using the MTT proliferation assay, the fabrics coated with the greatest phosphor ratio (15%) were examined for their cyctotoxic (in vitro) effects on normal epithelial human line cells (Soyingbe et al. 2018).

## Results and discussion

Morphological properties

Strontium aluminate ($SrAl_2O_4:Eu^{2+}$, $Dy^{3+}$) pigment was synthesized using the high-temperature solid-state technique (El-Newehy et al. 2022), and the pigment nanopowder was obtained by the top-down method (Camargos et al. 2021). Figure 2 shows TEM and selected area electron diffraction (SAED) images of strontium aluminate particles, demonstrating diameters of 2–12 nm. One of the recognized properties of nanomaterials is the capacity to produce transparent coats (Chae et al. 2003). In order to generate a colorless film onto cotton surface, the pigment nanoparticles must be uniformly disseminated in the screen-printing pastes or the spray-coating formulae to avoid the formation of aggregates (Chae et al. 2003).

The surface topography of treated textiles was analyzed. SEM images of the screen-printed and spray-coated fabrics with 10% phosphor content are shown in Fig. 3. The morphologies of the screen-printed textiles were identical to those of sprayed cottons. The surface topography of the coated textiles was drastically different from the blank fabric. In comparison to the blank cotton smooth surface, the treated fabrics ($SP_3$ and $SC_3$) were coated with the phosphor nanoparticles. It was found that the majority of the composite particles were

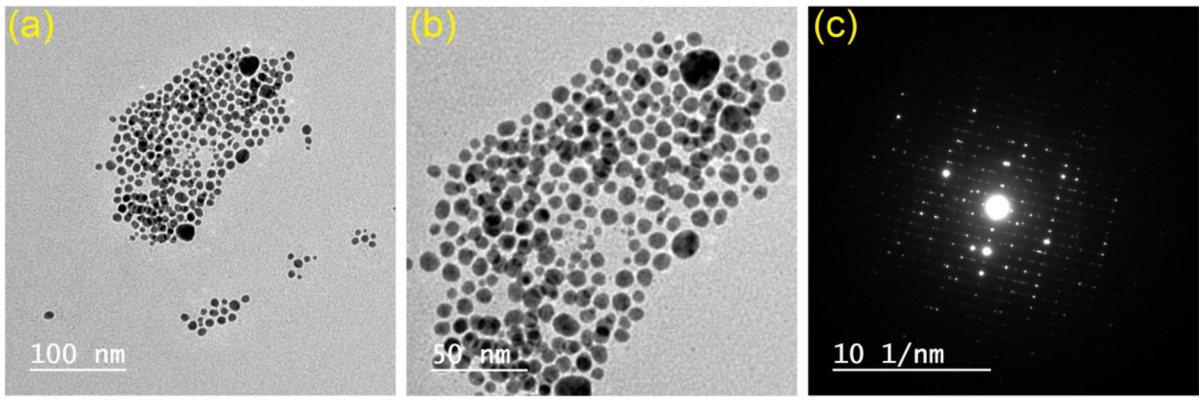


**Fig. 2** TEM **a–b**, and SAED **c** images of phosphor particles

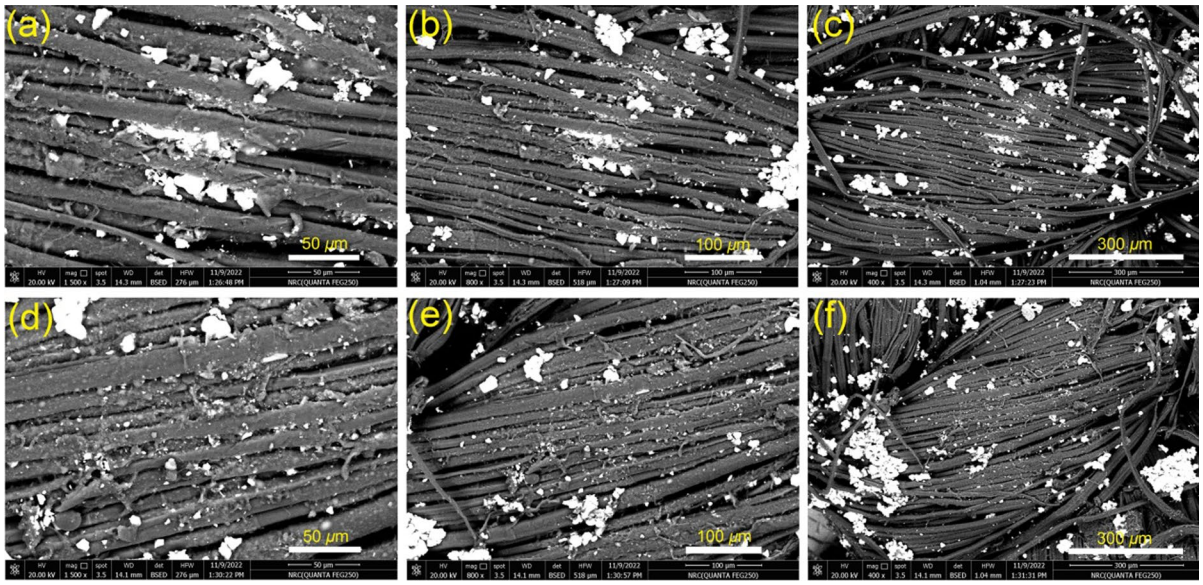


**Fig. 3** SEM images of SP3 (**a–c**), and SC3 (**d–f**)

entrapped in the spaces between the fibers. Cotton cellulose chains could successfully bind to phosphor molecules to result in a rougher surface. This demonstrates that the composite coats are capable of introducing a synergistic hydrophobicity in the development of a physical barrier on cotton surface, thereby preventing wettability. Elemental compositions as a percentage by weight are shown in Table 1 for three locations on cotton surface. Three different locations on the fabric surface were analyzed, showing that the pigment was evenly distributed over the cotton surface.

Carbon (C) and oxygen (O) are fundamental elemental components of the cellulose polymer that forms the basis of cotton textiles (Gao et al. 2021; Kibria et al. 2022; Subaihi et al. 2022; Wei et al. 2020). The reason that Si, P, Al, Sr, Eu, and Dy could be found using EDX analysis was because of the use of RTV, ammonium polyphosphate, lanthanide-activated strontium aluminate in low amounts. We also used XRF to gather data on the chemical composition of the phosphor-coated cottons, and the results are shown in Table 2. Due to its great sensitivity, EDX has been a reliable method for detecting trace

**Table 1** Elements identified by EDX (wt%) at different sites (A1, A2 and A3) on cotton surface

| Fabric | | C | O | Si | P | Al | Sr | Eu | Dy |
|---|---|---|---|---|---|---|---|---|---|
| SP1 | A1 | 50.77 | 25.02 | 15.27 | 7.10 | 1.06 | 0.44 | 0.27 | 0.13 |
| | A2 | 50.51 | 26.00 | 15.42 | 6.36 | 0.97 | 0.43 | 0.21 | 0.08 |
| | A3 | 50.53 | 25.04 | 15.50 | 7.21 | 0.88 | 0.42 | 0.23 | 0.09 |
| SP4 | A1 | 46.09 | 33.70 | 6.91 | 2.42 | 5.53 | 3.42 | 0.90 | 0.57 |
| | A2 | 46.61 | 34.20 | 6.04 | 2.79 | 5.32 | 3.67 | 0.83 | 0.55 |
| | A3 | 47.13 | 33.04 | 6.38 | 3.37 | 5.49 | 3.25 | 0.81 | 0.53 |
| SC1 | A1 | 64.40 | 26.80 | – | 6.25 | 1.44 | 0.63 | 0.29 | 0.19 |
| | A2 | 65.10 | 26.63 | – | 6.04 | 1.24 | 0.60 | 0.25 | 0.14 |
| | A3 | 64.81 | 26.86 | – | 6.00 | 1.34 | 0.62 | 0.20 | 0.17 |
| SC4 | A1 | 52.15 | 33.20 | – | 3.73 | 5.98 | 3.85 | 0.64 | 0.45 |
| | A2 | 52.70 | 33.03 | – | 3.94 | 5.69 | 3.57 | 0.65 | 0.41 |
| | A3 | 52.60 | 33.04 | – | 3.66 | 5.56 | 4.03 | 0.63 | 0.47 |

**Table 2** XRF results (wt%) of cotton substrates

| Element | $SP_1$ | $SC_1$ | $SP_4$ | $SC_4$ |
|---|---|---|---|---|
| Al | 65.04 | 48.41 | 65.35 | 54.17 |
| Sr | 34.96 | 22.23 | 33.02 | 26.06 |
| Si | – | 28.36 | – | 17.32 |
| Eu | 0 | 0 | 1.14 | 1.66 |
| Dy | 0 | 0 | 0.49 | 0.78 |

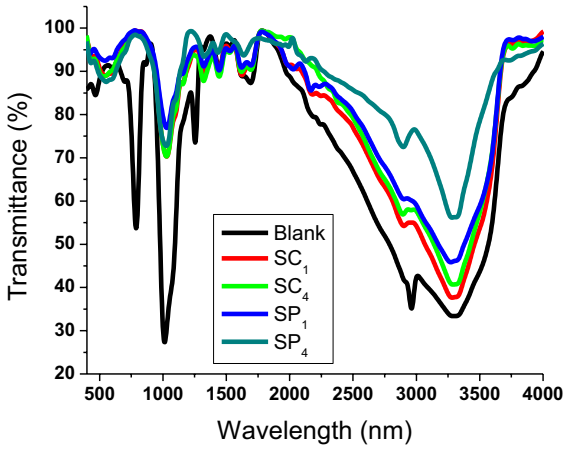


**Fig. 4** Infrared spectra of cotton fabrics

amounts of elements. The lowest elemental content that is detectable by XRF is 10 ppm (Ahmed et al. 2017). Thus, the XRF identification of elements is limited to aluminum and strontium. Owing to their extremely low amounts (< 10 ppm), Eu and Dy were undetectable. Hence, XRF failed to detect Dy and Eu in these coated cotton textiles because $SP_1$, $SP_2$, $SC_1$ and $SC_2$ had negligible amounts of phosphor. The molar ratios monitored by XRF and EDX on coated textiles were consistent with the molar ratios employed in the manufacture of pigment, printing pastes and spraying formulae.

Figure 4 demonstrates the infrared spectroscopy results of the binding process between the luminescent pigment and cotton. The peak at 2960 $cm^{-1}$ demonstrated the existence of aliphatic groups. A hydroxyl group could account for the 3310 $cm^{-1}$ absorption band. The stretch aliphatic intensity of blank cotton at 2960 $cm^{-1}$ was observed to diminish and shift to 2895 $cm^{-1}$ when the luminous pigment ratio was raised. The band monitored at 1013 $cm^{-1}$ is ascribed to the ether (C–O) stretch vibration of blank cotton, which was found to shift to 1025 $cm^{-1}$ when the luminous pigment ratio was raised. The $NH_4^+$ substituent was detected at 1440 $cm^{-1}$ due to the Exolit-AP422 agent. The bands of P–O–P, P–O, and P–OH were determined at 1253, 1326, and 1691 $cm^{-1}$, respectively. The peak at 551 $cm^{-1}$ was attributed to Si–O. The Sr–O, O–Al–O, and Al–O lattice vibrations were responsible for the bands determined at 422, 559, and 711 $cm^{-1}$, respectively. No considerable differences were detected in the infrared spectra of the screen-printed and spray-coated cotton samples at the same phosphor concentrations.

## Colorimetric results

The colorimetric properties before and after illumination with ultraviolet are summarized in Table 3. All

**Table 3** Colorimetric featuures of screen-printed and sprayed cotton fabrics at various phosphor ratios under daytime (DTL), and UV (UVL) lights

| Cotton | L* | | a* | | b* | | *K/S* | |
|---|---|---|---|---|---|---|---|---|
| | DTL | UVL | DTL | UVL | DTL | UVL | DTL | UVL |
| SP1 | 92.83 | 89.02 | −1.45 | −12.09 | 1.32 | 6.24 | 1.18 | 2.85 |
| SP2 | 91.64 | 87.44 | −1.39 | −12.74 | 1.43 | 6.20 | 1.26 | 3.04 |
| SP3 | 90.04 | 86.01 | −1.33 | −14.11 | 1.47 | 5.95 | 1.40 | 3.42 |
| SP4 | 88.72 | 84.29 | −1.25 | −18.23 | 1.51 | 5.24 | 1.47 | 4.06 |
| SC1 | 94.55 | 90.33 | −1.74 | −14.68 | 1.21 | 7.60 | 0.70 | 3.31 |
| SC2 | 94.17 | 88.02 | −1.69 | −17.09 | 1.27 | 6.40 | 0.81 | 4.72 |
| SC3 | 93.72 | 85.65 | −1.62 | −20.84 | 1.29 | 5.31 | 0.85 | 6.30 |
| SC4 | 93.25 | 83.29 | −1.53 | −22.38 | 1.32 | 4.30 | 0.88 | 7.24 |

*K/S* represents color strength, L* represents lightness from dark (0) to white (100), a* represents color ratios from red (+a*) to green (–a*), and b* represents color ratios from yellow (+b*) to blue (–b*)

coated cottons were almost as white as the cotton material was before the coating process began. As the concentration of the phosphor is increased, the *K/S* value rises somewhat in the pre-ultraviolet exposure situation, suggesting a level of color intensity comparable to that of blank cotton fabric, proving that the coated layer is transparent. The *K/S* value rises dramatically after UV exposure, suggesting a shift toward richer green color intensity associated with a higher phosphor concentration. The white color of the cotton fabric had L* of 95.02, a* of 0.03, and b* of 1.21. When the pigment ratio was increased on the coated layer, no observable differences were tracked in CIE Lab before they are exposed to UV light, confirming the transparency of the coated film. When the UV light is absorbed by the treated cotton, L* decreases, − a* increases, and + b* decreases, signifying a transition to a green color.

Photoluminescence analysis

Both of screen-printing and spray-coating technologies can be reported as efficient methods for incorporating inorganic pigment phosphors into cotton textiles, which allows for the creation of smart fabrics with photochromic and afterglow effects. However, the spraying process has been reported to be a fast, easy-to-use, more efficient than screen-printing technology, economical, affordable, and repeatable technology that preserves the textile aesthetic features. The phosphor nanoparticles were screen-printed and spray-coated onto cotton fabrics. All coated textiles showed traits of immediate and reversible photochromism upon exposure to UV. Turning off the UV source to reverse the fluorescence emission on the coated cotton material with pigment concentration of 1% was instantaneous. The garment decolorization and reversibility are slowed when using pigment concentrations > 1%, due to an afterglow emission caused by the absence of UV light. According to Fig. 5, the maximum absorption wavelength was determined to be 399 nm. As expected, a concentration-dependent excitation effect was reported by measuring the absorption wavelength intensity at 399 nm. Under UV light, the greatest emission wavelength was measured to be 516 nm, indicating a green emission (Fig. 6). When placed in a darkened room, the coated cotton fibers emit a greenish-yellow light. A time-dependent emission impact was confirmed by

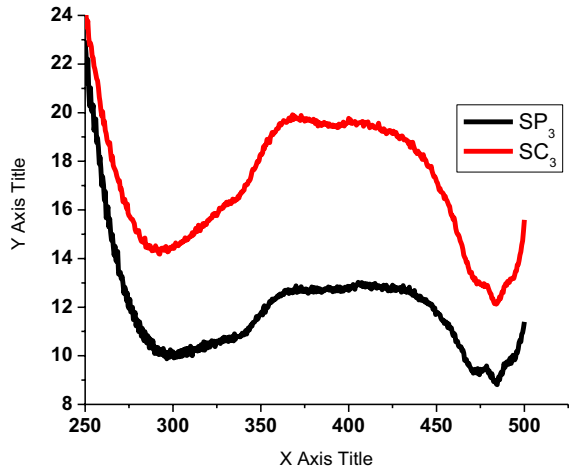


**Fig. 5** Excitation spectra of SP3 and SC3

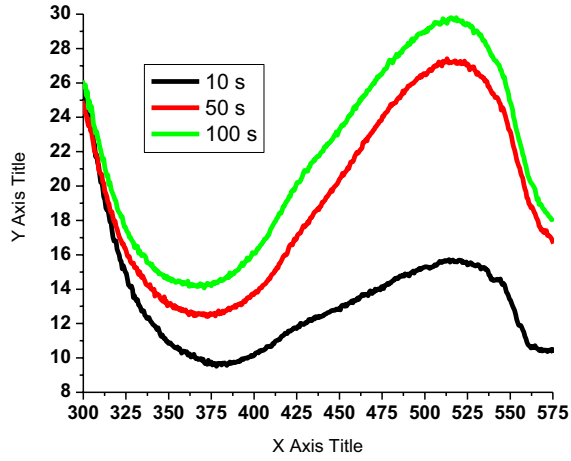


**Fig. 6** Emission of SC3 after UV-illumination for different time periods

a rise in the emission intensity with an increase in the exposure duration to ultraviolet light (10–100 s) as illustrated in Fig. 6.

The decay time have two different phases, the first of which is quite quick and the second of which is slower. Using $Dy^{3+}$ and $Eu^{2+}$, two lanthanide ions, allows for sustained afterglow emission. They are known as "trapping cations," because of their significant ability to delay photon emission (Abumelha 2021). Dense trapped photons produce an afterglow emission, the duration of which is dependent on the depth to which they were trapped.

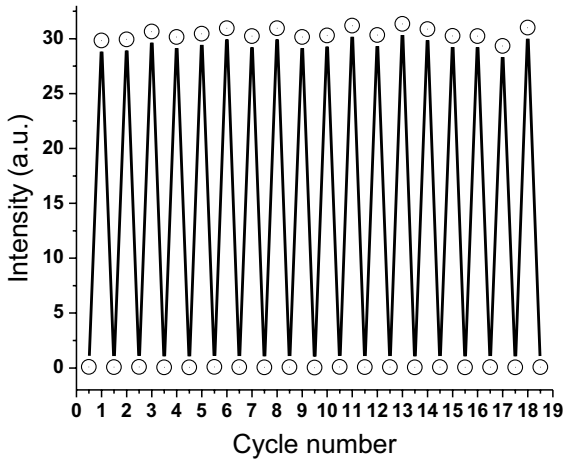


**Fig. 7** Emission intensities (516 nm) of SC3 before and after UV-illumination for 10 s

**Table 4** Contact angle (CA), UV blocking (UPF), and bend length (BL) and air-permeability (AP) of the screen-printed and spray-coated cotton fabrics

| Cotton | CA (°) | UPF | BL (cm) | | AP (cm3/cm2.s1) |
|---|---|---|---|---|---|
| | | | warp | weft | |
| Blank | – | – | 2.30 | 2.57 | 52.73 |
| SP1 | 109.0 | 65 | 2.71 | 2.93 | 51.62 |
| SP2 | 115.5 | 93 | 3.06 | 3.20 | 50.80 |
| SP3 | 119.3 | 134 | 3.35 | 3.58 | 50.23 |
| SP4 | 120.4 | 152 | 3.62 | 3.96 | 49.86 |
| SC1 | 137.5 | 98 | 2.50 | 2.72 | 51.84 |
| SC2 | 139.0 | 141 | 2.67 | 2.91 | 51.45 |
| SC3 | 143.1 | 177 | 2.88 | 2.95 | 51.07 |
| SC4 | 144.7 | 203 | 2.95 | 3.02 | 50.89 |

The cotton surface was illuminated with UV light for 5 min to produce green emission. The room was then darkened for an additional 60 min to enable the fabric to return to its natural white color. Numerous cycles of gradual re-illumination and fading were applied. The emission intensity was evaluated at the end of each cycle. Figure 7 demonstrates high reversibility, fatigue resistance and photostability.

## Hydrophobicity screening

Table 4 displays the contact angles of both screen-printed and spray-coated cotton textiles. Blank cotton has been known to be hydrophilic (Gao et al. 2021; Kibria et al. 2022; Subaihi et al. 2022; Wei et al. 2020). After treatment with phosphor at a concentration of 1%, the cotton fabric contact angle rises to about 109.0° ($SP_1$) and 137.5° ($SC_1$), signifying the development of more hydrophobic surface. Similar trends toward increased hydrophobicity were monitored in cotton fabrics when increasing the pigment ratio. Figure 8 shows the contact angle photographs of treated cotton fabrics; $SC_1$ and $SC_4$. The contact angle of $SC_4$ reached 144.7°, which is quite higher than the contact angle measured for screen-printed cotton fabric ($SP_4$) at 120.4°. Thus, the spray-coating technology works well enough to make superhydrophobic cotton textiles. By creating an additional barrier between water and treated fabric surface, the incorporation of phosphor nanoparticles greatly improved hydrophobicity. Fabrics with a higher phosphor concentration had a rougher surface because the nanoparticles of phosphor filled the spaces between the cotton fibers (Ibarhiam et al. 2022). Thus, the lower amounts of phosphor particles deposited onto cotton surface by spraying technology have showed improved hydrophobicity. On the other hand, the screen-printing technology has been known to deposit higher amounts of the phosphor nanoparticles, which lower surface roughness owing to decreasing the gaps

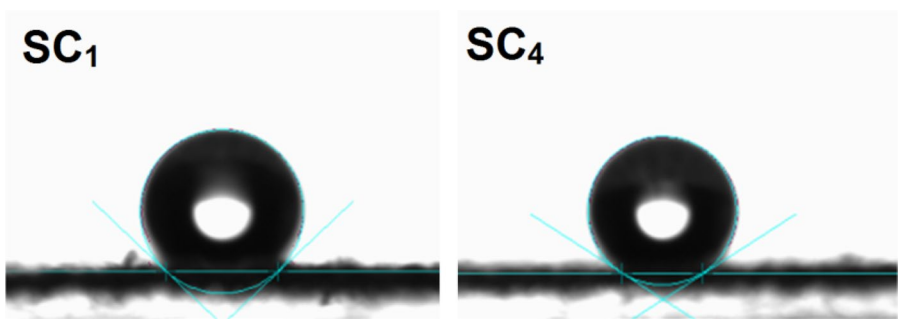


**Fig. 8** Photographs of the contact angles of treated cotton fabrics; SC1 and SC4

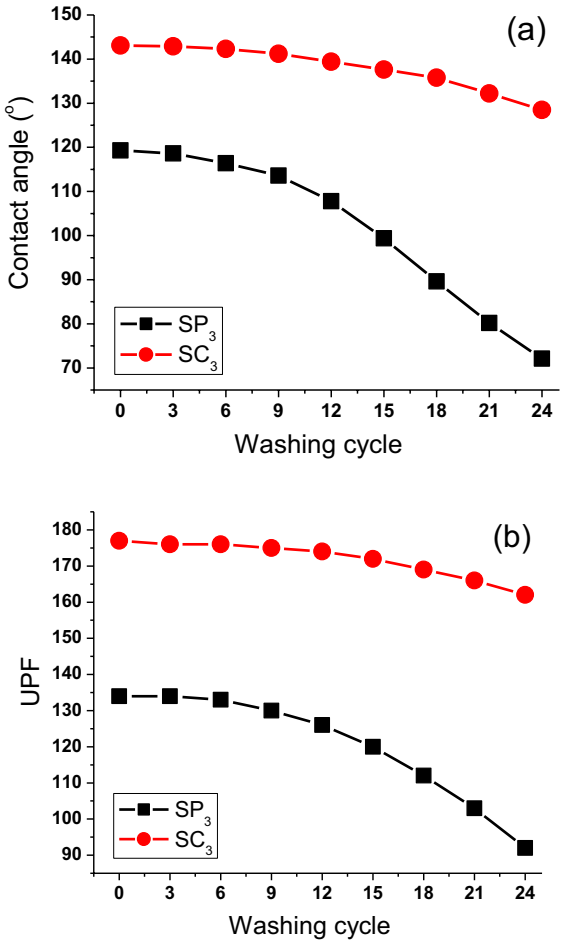


**Fig. 9** Effect of washing cycles on contact angle (**a**), and ultraviolet protection (**b**)

between the phosphor particles, and consequently decreased the contact angles (Ibarhiam et al. 2022). As shown in Fig. 9a, the contact angle was monitored to decrease as the number of washing cycles increased. When the number of laundry process reached 24 cycles, the contact angle decreased from 143.1° to 128.5° for the spray-coated samples, and considerably decreased from 119.3° to 72.1° for the screen-printed textiles.

## UV-protection and comfort screening

Table 4 displays the UPF values to assess the ultraviolet protection of cotton textile. Higher UPF was detected in the phosphor-coated cotton fabrics compared to the blank cotton. This can be assigned to the strong UV absorbance activity of the phosphor nanoparticles to effective block the ultraviolet rays. However, the screen-printed cotton samples showed a better UV-protection as compared to the sprayed samples. This can be assigned to the higher phosphor density deposited by the screen-printing technology as compared to spray-coating technology. The ultraviolet protection decreased as the number of washing cycles increased as shown in Fig. 9b. After 24 laundry, the UPF value decreased from 177 to 162 for the spray-coated samples, and considerably decreased from 134 to 162 for the screen-printed textiles. Table 4 displays the results for air permeability and bend length. The fabrics with a higher phosphor ratio were somewhat less air permeable and had a lower bending length. However, the spray-coated fabrics showed better air permeable and bending length as compared to the screen-printed samples due to the higher phosphor density immobilized by screen-printing as compared to spray-coating. Both screen-printed and spray-coated textiles displayed an improved durability against perspiration, crocking, light, and laundering (Table 5). However, the spray-coated fabrics showed a slightly higher colorfastness properties as compared to the screen-printed samples.

## Flame-retardant screening

Phosphorus-containing materials can be reported as environmentally friendly and efficient flame resistant agents (Abdelrahman and Khattab 2019). Ammonium polyphosphate has been reported as formaldehyde-free alternative to the commercially available Pyrovatex fire-resistant agent (Wu et al. 2022). Figure 10 displays the vertical flammability testing chamber. The blank cotton failed the flammability test and was completely burnt. The flame-resistant properties of the finished cottons were remarkably improved as shown in Table 6. The char length was monitored to slightly decrease as the phosphor content increased. When raising the phosphor ratio, the char length was slightly decreased from 47 to 42 mm for the screen-printed samples, and decreased from 43 to 37 mm for the spray-coated textiles. The fire-retardant activity of the treated fabrics was stable over 24 laundry cycles.

The LOI method was also used to test cotton fabrics by reporting the minimum concentration of oxygen that supports the fabric combustion (Abd El-Wahab et al. 2020). It has been known that there

**Table 5** Colorfastness screening of finished cottons

| Cotton | Crocking | | Washing | | Perspiration | | | | Light |
|---|---|---|---|---|---|---|---|---|---|
| | Dry | Wet | Alt | St | Acid | | Base | | |
| | | | | | Alt | St | Alt | St | |
| SP1 | 4 | 3–4 | 4 | 4 | 4–5 | 4–5 | 3–4 | 4 | 6 |
| SP2 | 4 | 3–4 | 4 | 4 | 4–5 | 4–5 | 4 | 4 | 6 |
| SP3 | 4 | 4 | 4 | 4 | 4–5 | 4–5 | 4 | 4 | 6 |
| SP4 | 4 | 4 | 4 | 4 | 4 | 4 | 3–4 | 3–4 | 6 |
| SC1 | 4–5 | 4–5 | 4–5 | 4–5 | 4–5 | 4–5 | 4–5 | 4–5 | 6–7 |
| SC2 | 4–5 | 4–5 | 4–5 | 4–5 | 4–5 | 4–5 | 4–5 | 4–5 | 6–7 |
| SC3 | 4–5 | 4–5 | 4–5 | 4–5 | 4–5 | 4–5 | 4–5 | 4–5 | 6–7 |
| SC4 | 4–5 | 4–5 | 4 | 4 | 4–5 | 4–5 | 4 | 4 | 6 |

*Alt* color alteration, **St* cotton staining

**Fig. 10** Vertical flammability testing chamber

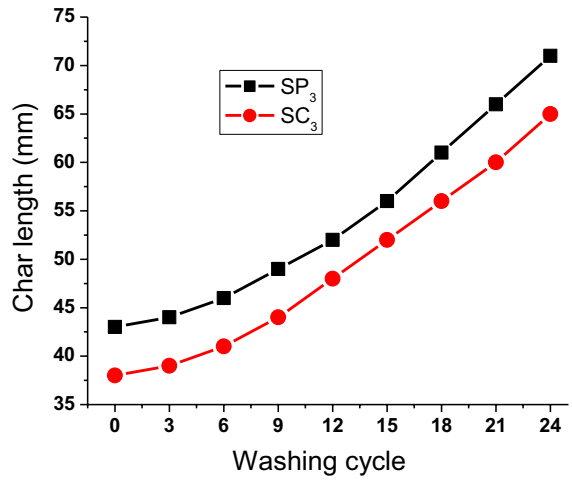


**Fig. 11** Effect of washing cycles on cotton flammability

**Table 6** Impact of phosphor ratio on cotton flammability

| Cotton | C.L. (mm) | C.W. (mm) | LOI (%) |
|---|---|---|---|
| Blank | Burnt completely | | 17 |
| SP1 | 47 | 18 | 39 |
| SP2 | 45 | 18 | 40 |
| SP3 | 43 | 18 | 42 |
| SP4 | 42 | 17 | 42 |
| SC1 | 43 | 17 | 51 |
| SC2 | 40 | 17 | 52 |
| SC3 | 38 | 17 | 54 |
| SC4 | 37 | 17 | 55 |

*C.L.* represents the char length (mm), *C.W.* represents the char width (mm), *LOI* represents limited oxygen index (%)

is about ~ 21% oxygen in atmospheric air. A material with LOI value less than 21% readily burns under atmospheric conditions, whereas a material with LOI value in the range of 21–28% displays "slow burning" (Abd El-Wahab et al. 2020). The LOI value of blank cotton was 17%. As compared to blank cotton fabric, the finishing process of cotton fibers with ammonium polyphosphate (flame-retardant agent) provided fire-resistant activity as shown in Table 6. The LOI value was monitored to slightly increase as the phosphor content increased. However, the spray-coated textiles have showed better self-extinguishing properties as compared to the screen-printed samples.

**Table 7** Antibacterial activity of phosphor-finished cotton fabrics versus *S. typhimurium* (S.t.), and *S. aureus* (S.a.)

| Number of washes | Bacterial species | Bacteria reduction (%) | | | |
|---|---|---|---|---|---|
| | | $SP_1$ | $SP_4$ | $SC_1$ | $SC_4$ |
| 0 | S.a | 32 ± 1.0 | 37 ± 1.2 | 43 ± 1.1 | 48 ± 1.4 |
| | S.t | 39 ± 1.2 | 42 ± 1.0 | 46 ± 1.2 | 57 ± 1.2 |
| 5 | S.a | 24 ± 1.5 | 27 ± 1.4 | 31 ± 1.1 | 39 ± 1.3 |
| | S.t | 25 ± 1.1 | 28 ± 1.2 | 33 ± 1.1 | 45 ± 1.3 |
| 10 | S.a | 13 ± 1.5 | 15 ± 1.9 | 22 ± 1.6 | 27 ± 1.0 |
| | S.t | 17 ± 1.7 | 20 ± 1.6 | 24 ± 1.8 | 35 ± 1.5 |
| 15 | S.a | 11 ± 1.6 | 13 ± 1.3 | 18 ± 1.4 | 21 ± 1.1 |
| | S.t | 15 ± 1.0 | 18 ± 1.3 | 20 ± 1.0 | 24 ± 1.0 |

The flame-retardant durability of the cotton fabric ($SC_3$) was studied over several laundry cycles. The char length was measured after different laundry cycles as illustrated in Fig. 11. It increased with raising the number of the laundry cycles to withstand 24 washes. However, the fabric was completely burned after the 24 washing cycles.

Biological properties

The antibacterial characteristics of the phosphor-finished cotton textiles were evaluated after they were washed up to 15 cycles using the standardized AATCC (2007:193) protocol (Shen et al. 2022). The finished cottons showed antibacterial activity against *S. typhimurium* and *S. aureus* as described in Table 7. The cotton material was coated with varying quantities of the pigment nanoparticles. Since blank cotton fabric does not include any antimicrobial agents, it was unable to eliminate the bacteria that were tested. The finishing of cotton with a phosphor concentration of 1% was effective in killing bacteria adhering to the fabric. When the phosphor ratio rose, the amount of bacteria was highly reduced. The greatest bacterial decrease observed for cotton fabrics with 15% of phosphor nanoparticles. The number of germs was shown to drop significantly after 15 washes. It is possible that the antibacterial activity of the finished cottons is due to the liberation of active ions through the physical contact between the bacteria membrane and pigment particles (Gu et al. 2021).

**Table 8** Cytotoxicity of phosphor-finished cotton fabrics (phosphor content of 15%) using epithelial line cells (100 µg/mL)

| Toxicity (%) | IC-90 (µg/mL) | IC-50 (µg/mL) | Cotton |
|---|---|---|---|
| SP4 | – | – | 1.3 |
| SC4 | – | – | 1.0 |
| DMSO | – | – | 1 |
| Control (−ve) | – | – | 0 |

Using the MTT proliferation assay, he cytotoxic effects of the produced phosphor-finished cotton textile substrates were tested in vitro on normal epithelial human line cells (Soyingbe et al. 2018). Table 8 displays that even at the greatest pigment content (15%), the cytotoxicity of the finished cotton fabrics was exceptionally low.

## Conclusions

Screen-printed and spray-coated cotton fabrics finished with lanthanide-doped aluminate showed UV-blocking, flame-retardant, water-repellency, dual-mode photochromism, antibacterial activity. Images captured by TEM were used to quantify phosphor particle sizes in the range of 2–12 nm. The ammonium polyphosphate agent was applied as an environmentally benign flame-retardant. On the other hand, the environmentally friendly silicone rubber was applied as a hydrophobic agent. The strontium aluminate particles were directly coated onto cotton surface to produce a smart composite film with enhanced water-repellency, flame-retardant, antibacterial activity and UV blocking as compared to blank cotton. Greenish emission was determined at 516 nm after being excited at 399 nm. To achieve a transparent nanocomposite layer on fabric surface, the phosphor particles must be well-dispersed in either the screen-printing pastes or the spray-coating formulae to prevent the formation of aggregates. For the phosphor ratio of 1%, intense green fluorescence was detected in UV light, while the pigment ratio greater than 1% showed a long-lasting greenish-yellow afterglow. The multifunctional characteristics of the treated textiles were found to improve by increasing the strontium

aluminate ratio. The contact angle values demonstrated an increase from 109.0° (1%; $SP_1$) to 120.4° (15%; $SP_4$) for the screen-printed fabrics, and from 137.5° (1%; $SC_1$) to 144.7° (15%; $SC_4$) for the spray-coated fabrics. Thus, the 15% phosphor ratio cloth developed by the spray-coating technology was found to have the best hydrophobic characteristics. The flame-retardant property of cottons was enhanced after treatment with ammonium polyphosphate. When increasing the phosphor content, the char length was slightly decreased from 47 to 42 mm for the screen-printed fabrics, and decreased from 43 to 37 mm for the spray-coated fabrics. The flame-retardant property of the fabrics treated with the ammonium polyphosphate agent showed stability over 24 laundry cycles. At the maximum ratio of strontium aluminate (15%), the cytotoxicity analysis of the present finished cotton was remarkably low to man skin. The colorfastness of fabrics spray-coated with strontium aluminate was much higher than the screen-printed fabrics. Due to its remarkable durability and photostability, the current method is well-suited for use in a wide range of niche markets, including military camouflage, security encoding, brand protection, and smart packaging.

**Acknowledgements** National Research Centre of Egypt is acknowledged for the financial support of the current research under project number (12010206).

**Author contributions** EA, DM, TAK: methodology, investigation, writing—original draft preparation; MSA, TMH, TAK: resources, data curation, writing—reviewing, formal analysis. TMH, EA, MSA: supervision, visualization, conceptualization, formal analysis, supervision, writing—reviewing and editing.

**Funding** Open access funding provided by The Science, Technology & Innovation Funding Authority (STDF) in cooperation with The Egyptian Knowledge Bank (EKB).

**Data availability** All relevant data are within the manuscript and available from the corresponding author upon request.

**Declarations**

**Conflict of interest** All the authors hereby declare that they do not have any conflict of interest about this manuscript.

**Ethical approval** Not applicable.

**Consent to participate** All authors were participated in this work.

**Consent for publication** All authors agree to publish.



## References

Abd El-Wahab H, Abd El-Fattah M, El-Alfy HMZ, Owda ME, Lin L, Hamdy I (2020) Synthesis and characterisation of sulphonamide (Schiff base) ligand and its copper metal complex and their efficiency in polyurethane varnish as flame retardant and antimicrobial surface coating additives. Prog Org Coat 142:105577

Abdelrahman MS, Khattab TA (2019) Development of one-step water-repellent and flame-retardant finishes for cotton. ChemistrySelect 4(13):3811–3816

Abou-Melha K (2022) Preparation of photoluminescent nanocomposite ink toward dual-mode secure anti-counterfeiting stamps. Arab J Chem 15(2):103604

Abumelha HM (2021) Simple production of photoluminescent polyester coating using lanthanide-doped pigment. Luminescence 36(4):1024–1031

Adamu BF (2022) Permeability and moisture management properties of denim fabric made from cotton, spandex, and polyester. J Inst Eng India A 103(2):253–258

Ahmed N, Ahmed R, Rafiqe M, Baig MA (2017) A comparative study of Cu–Ni alloy using LIBS, LA-TOF, EDX, and XRF. Laser Part Beams 35(1):1–9

Ahmed H, Abdelrahman MS, Al-Balakocy NG, Wen Z, Khattab TA (2022) Preparation of photochromic and photoluminescent nonwoven fibrous mat from recycled polyester waste. J Polym Environ 30(12):5239–5251

Alsharief HH, Al-Hazmi GA, Alzahrani SO, Almahri A, Alamrani NA, Alatawi NM, El-Metwaly NM (2022) Immobilization of strontium aluminate nanoparticles onto plasma-pretreated nonwoven polypropylene fibers by screen-printing toward photochromic textiles. J Mater Res Technol 20:3146–3157

Bao B, Fan J, Wang W, Yu D (2020) Photochromic cotton fabric prepared by spiropyran-ternimated water polyurethane coating. Fibers Polym 21(4):733–742

Camargos CH, Rezende CA (2021) Antisolvent versus ultrasonication: bottom-up and top-down approaches to produce lignin nanoparticles (LNPs) with tailored properties. Int J Biol Macromol 193:647–660

Chae SY, Park MK, Lee SK, Kim TY, Kim SK, Lee WI (2003) Preparation of size-controlled TiO2

nanoparticles and derivation of optically transparent photocatalytic films. Chem Mater 15(17):3326–3331
Chen G, Li Y, Bick M, Chen J (2020) Smart textiles for electricity generation. Chem Rev 120(8):3668–3720
De Falco F, Guarino V, Gentile G, Cocca M, Ambrogi V, Ambrosio L, Avella M (2019) Design of functional textile coatings via non-conventional electrofluidodynamic processes. J Colloid Interface Sci 541:367–375
El-Naggar ME, Ali OAA, Saleh DI, Abu-alnja KM, Mnsour AAM, Abu-Saied MA, Khattab TA (2022) Production of smart cotton-nickel blend fibers using functional polymers comprising ammonium polyphosphate and silicone rubber. Fibers Polym 23(6):1560–1571
El-Newehy MH, Kim HY, Khattab TA, El-Naggar ME (2022) Development of highly photoluminescent electrospun nanofibers for dual-mode secure authentication. Ceram Int 48(3):3495–3503
Fan J, Bao B, Wang Z, Xu R, Wang W, Yu D (2020) High tristimulus response photochromic cotton fabrics based on spiropyran dye by thiol-ene click chemistry. Cellulose 27(1):493–510
Fan S, Lam Y, Yang J, Bian X, Xin JH (2022) Development of photochromic poly (azobenzene)/PVDF fibers by wet spinning for intelligent textile engineering. Surf Interfaces 34:102383
Fang Y, Chen G, Bick M, Chen J (2021) Smart textiles for personalized thermoregulation. Chem Soc Rev 50:9357–9374
Faruk MO, Ahmed A, Jalil MA, Islam MT, Adak B, Hossain MM, Mukhopadhyay S (2021) Functional textiles and composite based wearable thermal devices for Joule heating: progress and perspectives. Appl Mater Today 23:101025
Gao D, Li X, Li Y, Lyu B, Ren J, Ma J (2021) Long-acting antibacterial activity on the cotton fabric. Cellulose 28(3):1221–1240
Gao C, Zhang Y, Jiang B, Xi R, Zhu K, Wang Y, Xu W, Song D (2022a) Construction of durable and original color constancy photochromic cotton fabrics by a facile esterification strategy. Ind Crop Prod 189:115783
Gao H, Liu G, Cui C, Wang M, Gao J (2022b) Preparation and properties of a polyurethane film based on novel photochromic spirooxazine chain extension. New J Chem 46(19):9128–9137
Gong F, Meng C, He J, Dong X (2018) Fabrication of highly conductive and multifunctional polyester fabrics by spray-coating with PEDOT: PSS solutions. Prog Org Coat 121:89–96
Gu X, Xu Z, Gu L, Xu H, Han F, Chen B, Pan X (2021) Preparation and antibacterial properties of gold nanoparticles: a review. Environ Chem Lett 19(1):167–187
He Z, Bao B, Fan J, Wang W, Yu D (2020) Photochromic cotton fabric based on microcapsule technology with antifouling properties. Colloids Surf A Physicochem Eng Asp 594:124661
Hu Q, Huang J, Wang J, Tan R, Feng Y, Xu X, Li J, Lu Y, Song W (2022) A universal green coating strategy on textiles for simultaneous color and thermal management. J Mater Sci 57(25):11477–11490
Ibarhiam SF, Alzahrani SO, Snari RM, Aldawsari AM, Alhasani M, Saad F, El-Metwaly NM (2022) Novel multifunctional acrylic paint from sugarcane bagasse: photoluminescence, photochromism, hydrophobicity and anticorrosion. Mater Today Commun 33:104703
Khattab TA, Rehan M, Hamouda T (2018) Smart textile framework: Photochromic and fluorescent cellulosic fabric printed by strontium aluminate pigment. Carbohydr Polym 195:143–152
Khattab TA, Tolba E, Gaffer H, Kamel S (2021) Development of electrospun nanofibrous-walled tubes for potential production of photoluminescent endoscopes. Ind Eng Chem Res 60(28):10044–10055
Kibria G, Repon M, Hossain M, Islam T, Jalil MA, Aljabri MD, Rahman MM (2022) UV-blocking cotton fabric design for comfortable summer wears: factors, durability and nanomaterials. Cellulose 29(14):7555–7585
Lamas-Ardisana PJ, Martínez-Paredes G, Añorga L, Grande HJ (2018) Glucose biosensor based on disposable electrochemical paper-based transducers fully fabricated by screen-printing. Biosens Bioelectron 109:8–12
Meena JS, Choi SB, Jung SB, Kim JW (2022) Recent progress of Ti3C2Tx-based MXenes for fabrication of multifunctional smart textiles. Appl Mater Today 29:101612
Roach DJ, Yuan C, Kuang X, Li VCF, Blake P, Romero ML, Hammel I, Yu K, Qi HJ (2019) Long liquid crystal elastomer fibers with large reversible actuation strains for smart textiles and artificial muscles. ACS Appl Mater Interfaces 11(21):19514–19521
Shen L, Jiang J, Liu J, Fu F, Diao H, Liu X (2022) Cotton fabrics with antibacterial and antiviral properties produced by a simple pad-dry-cure process using diphenolic acid. Appl Surf Sci 600:154152
Shi Q, Sun J, Hou C, Li Y, Zhang Q, Wang H (2019) Advanced functional fiber and smart textile. Adv Fiber Mater 1(1):3–31
Soyingbe OS, Mongalo NI, Makhafola TJ (2018) In vitro antibacterial and cytotoxic activity of leaf extracts of *Centella asiatica* (L.) Urb, *Warburgia salutaris* (Bertol. F.) Chiov and *Curtisia dentata* (Burm. F.) CA Sm-medicinal plants used in South Africa. BMC Complement Altern Med 18(1):1–10
Subaihi A, Al-Qahtani SD, Attar R, Alkhamis K, Alzahrani HK, Alhasani M, El-Metwaly NM (2022) Preparation of fluorescent cotton fibers with antimicrobial activity using lanthanide-doped pigments. Cellulose 29(11):6393–6404
Sun M, Lv J, Xu H, Zhang L, Zhong Y, Chen Z, Sui X, Wang B, Feng X, Mao Z (2020) Smart cotton fabric screen-printed with viologen polymer: photochromic, thermochromic and ammonia sensing. Cellulose 27(5):2939–2952
Tadesse MG, Harpa R, Chen Y, Wang L, Nierstrasz V, Loghin C (2019) Assessing the comfort of functional fabrics for smart clothing using subjective evaluation. J Ind Text 48(8):1310–1326
Tat T, Chen G, Zhao X, Zhou Y, Xu J, Chen J (2022) Smart textiles for healthcare and sustainability. ACS Nano 16(9):13301–13313
Thite AG, Krishnanand K, Sharma DK, Mukhopadhyay AK (2018) Multifunctional finishing of cotton fabric by electron beam radiation synthesized silver nanoparticles. Radiat Phys Chem 153:173–179
Wang L, Shi B, Zhao H, Qi X, Chen J, Li J, Shang Y, Fu KK, Zhang X, Tian M, Qu L (2022) 3D-printed

parahydrophobic functional textile with a hierarchical nanomicroscale structure. ACS Nano 16(10):16645–16654

Wei DW, Wei H, Gauthier AC, Song J, Jin Y, Xiao H (2020) Superhydrophobic modification of cellulose and cotton textiles: methodologies and applications. J Bioresour Bioprod 5(1):1–15

Wongphan P, Harnkarnsujarit N (2020) Characterization of starch, agar and maltodextrin blends for controlled dissolution of edible films. Int J Biol Macromol 156:80–93

Wu X, Gou T, Zhao Q, Chen L, Wang P (2022) High-efficiency durable flame retardant with ammonium phosphate ester and phosphine oxide groups for cotton cellulose biomacromolecule. Int J Biol Macromol 194:945–953

Yang Y, Li M, Fu S (2021) Screen-printed photochromic textiles with high fastness prepared by self-adhesive polymer latex particles. Prog Org Coat 158:106348

Yuan J, Yuan Y, Tian X, Wang H, Liu Y, Feng R (2019) Photoswitchable boronic acid derived salicylidenehydrazone enabled by photochromic spirooxazine and fulgide moieties: multiple responses of optical absorption, fluorescence emission, and quadratic nonlinear optics. J Phys Chem C 123(49):29838–29855

Zampini G, Ortica F, Cannavale A, Latterini L (2022) Spirooxazine loading effects on the photochromism of polymer films. Dyes Pigment 210:111018

Zhang M, Zhao M, Jian M, Wang C, Yu A, Yin Z, Liang X, Wang H, Xia K, Liang X, Zhai J (2019) Printable smart pattern for multifunctional energy-management E-textile. Matter 1(1):168–179